

# Load testing of 30-year-old AASHTO Type III highway bridge girders

**B. E. Ross, M. H. Ansley,  
and H. R. Hamilton III**

Four Type III American Association of State Highway and Transportation Officials (AASHTO) girders were salvaged as part of recent highway and bridge reconstruction along Interstate 75 (I-75) in Florida. The Florida Department of Transportation (FDOT) recovered the girders for testing. Test results add to the database of full-scale shear tests, such as those conducted by Ma et al.,<sup>1</sup> Shahawy et al.,<sup>2</sup> and others.<sup>3-7</sup> Unique aspects of these girders include light shear reinforcement, no confinement reinforcement, end diaphragms, a deck comprising precast and cast-in-place concrete, and a 30-year service life.

The salvaged girders were tested in three-point bending with shear span-to-depth ratios  $a/d$  ranging from 1.2 to 5.4. The experimental program was conducted to evaluate the behavior, failure mode, and capacity of existing AASHTO Type III girders loaded at varying  $a/d$ . Development lengths of prestressing strands and effects of end region detailing were of particular interest for girders tested using smaller  $a/d$ , while mode of failure was of particular interest for girders tested using larger  $a/d$ . The bridge deck was constructed using pretensioned, precast concrete slabs with a cast-in-place concrete topping. The effect of the deck system on the behavior of the girders was also of interest. The experimental results are compared to methods currently used to predict shear and flexural capacity.

## Girder acquisition and condition

Four girders were salvaged from a highway overpass bridge 10 mi (16 km) from the Gulf of Mexico in Sarasota County, Florida. The bridge was built in 1979 using AASHTO Type III prestressed concrete girders that were

- Four AASHTO Type III girders were salvaged from a 30-year-old bridge in Sarasota County, Fla., and tested in three-point bending at shear span-to-depth ratios ranging from 1.2 to 5.4.
- Experimental capacities were compared with sectional models, strut-and-tie models, and the end-region requirement for longitudinal reinforcement in the AASHTO LRFD specifications.
- The results indicate that the girders suffered no ill effects from age or exposure over the 30-year service life.

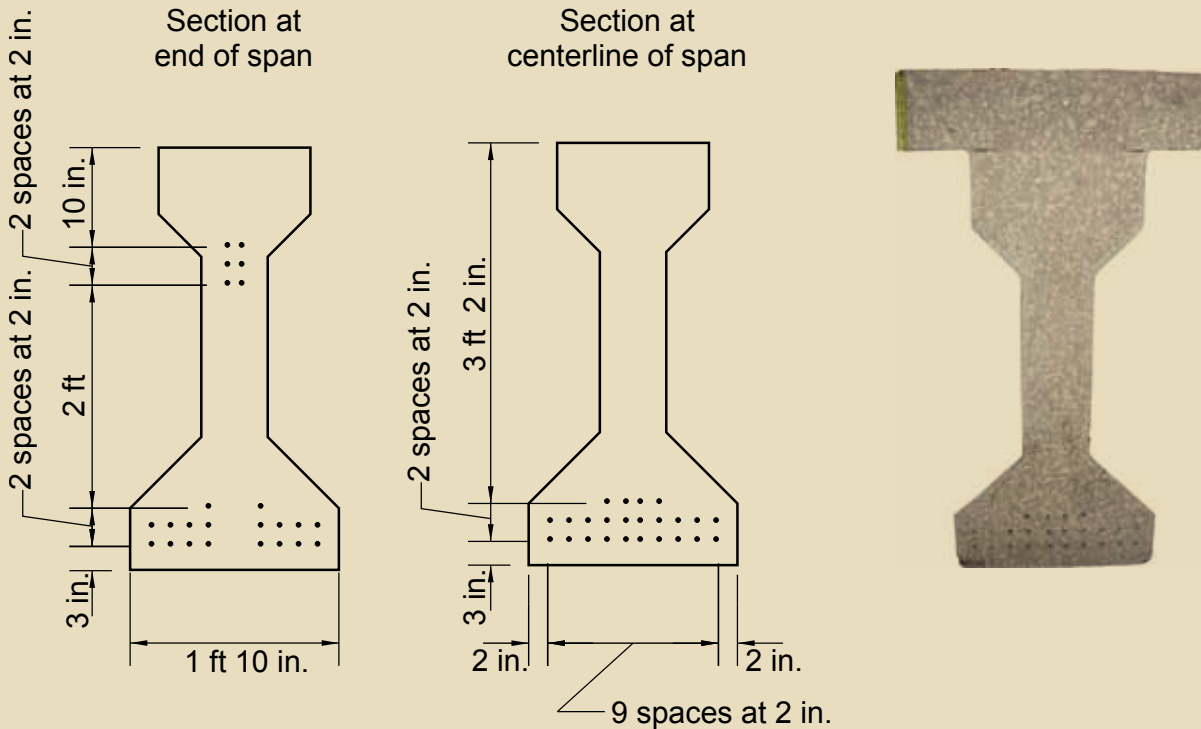


**Figure 1.** Test specimens were salvaged AASHTO Type III girders with harped and straight strands. Note: 1 in. = 25.4 mm; 1 ft = 0.305 m.

spaced at 10.5 ft (3.2 m) and had a span length of approximately 60 ft (18 m). The girders were originally designed using the 1973 edition of the AASHTO *Standard Specifications for Highway Bridges*.<sup>8</sup> The end diaphragms and bridge deck were saw cut to facilitate removal. The girders were transported by truck to the testing laboratory.

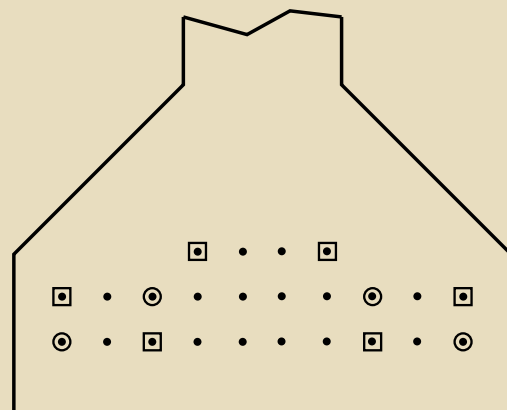
The latest inspection of the bridge had been completed in February 2007. The overall ratings for the bridge deck and superstructure were good. The bare concrete deck was described in FDOT report BD 545-56<sup>7</sup> to “have a few repaired areas, there are few spalls/delaminations in the deck surface or underside and the only cracking is superficial or surface map cracking.” The girders were found to have little or no visible deterioration but did have minor cracking and some discoloration due to efflorescence. The report indicated that the cracking was not anticipated to affect strength or serviceability.

### Girder details

The original construction drawings indicated that the girders were prestressed with twenty-four 0.5-in.-diameter (13 mm), 250 ksi (1720 MPa) stress-relieved strands tensioned to 28.9 kip (129 kN). Tension testing of strand samples, however, indicated that the strands had an ultimate tensile strength of 286 ksi (1970 MPa). The six innermost strands were harped with depression points at approximately 29.75 ft (9.07 m) from each end (**Fig. 1**).

Ten strands were debonded for either 1 ft (0.3 m) or 2 ft (0.60 m) from the ends (**Fig. 2**).

The end region of the girders was reinforced with longitudinal and transverse mild steel (**Fig. 3**). Longitudinal mild steel consisted of continuous N-bars in the top flange and L-bars in the end regions. Transverse K1 and K2 bars extended above the top flange of the beam into the deck to



- Strands debonded 24 in. from end of beam
- Strands debonded 12 in. from end of beam

**Figure 2.** Locations of strand debonding. Note: 1 in. = 25.4 mm.

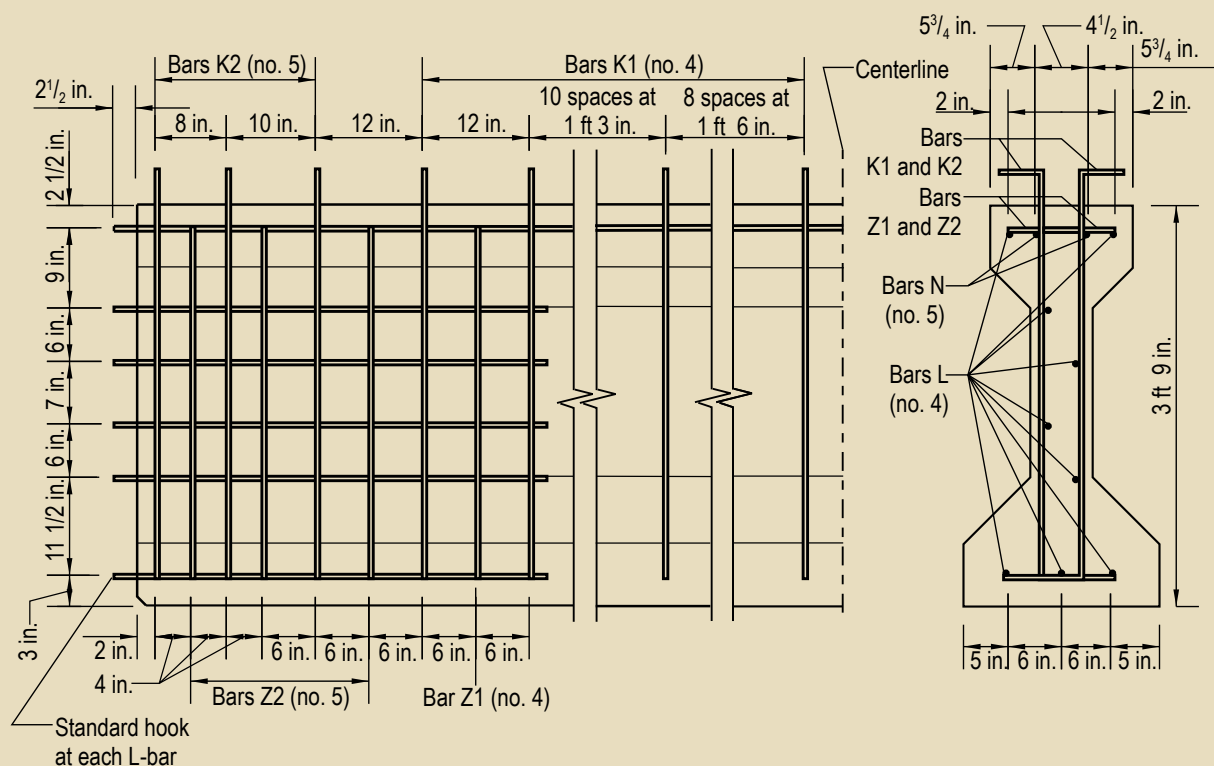


**Figure 3.** Girders contained horizontal and vertical mild steel reinforcement. Note: no. 4 = 13M; no. 5 = 16M; 1 in. = 25.4 mm; 1 ft = 0.305 m.

provide horizontal shear transfer between the girder and the deck. The Z1 and Z2 bars provided additional transverse reinforcement in the end regions. The transverse bars were always installed in pairs along the length of the beam.

The 7-in.-thick (180 mm) deck consisted of precast, prestressed concrete panels spanning between girders with a 7-in.-thick cast-in-place concrete topping (Fig. 4). During demolition, the deck was saw cut such that a 28-in.-wide (710 mm) section remained with each girder. The figures show average values because the deck dimensions varied slightly. The precast concrete panel was corrugated to improve the bond with the topping and was prestressed with  $\frac{3}{8}$ -in.-diameter (9.5 mm) strand placed in the panel span direction (transverse to the girder). The precast concrete panels were bearing on roofing paper and had a bearing length of 2.5 in. (64 mm). The topping was reinforced longitudinally with no. 7 (22M) bars and transversely with no. 5 (16M) bars.

A 28-in.-wide (710 mm) section of the end diaphragm was retained at each end of the girders. The cast-in-place concrete end diaphragm was 8 in. (203 mm) thick and was reinforced with horizontal and vertical bars at each face (Fig. 5).

To determine material properties, samples of the concrete, stirrups, and prestressing strands were taken after the girders were tested. The samples were tested, revealing the

following material properties: 5630 psi (38.3 MPa) compressive strength of web concrete, 4960 psi (34.2 MPa) compressive strength of deck concrete, 57 ksi (390 MPa) yield strength of mild steel, and 286 ksi (1970 MPa) tensile strength of prestressing strands. No significant corrosion of the prestressing strand or mild steel was noted during sampling.

FDOT report BD 545-56 has additional information on the girder acquisition, details, and materials.

## Test setup and procedures

Girders were tested using a three-point loading scheme with five different  $a/d$  ranging from 1.2 to 5.4. Two of the girders were tested at both ends, and the other two girders were tested at only one end, resulting in a total of six tests. A unique designation was given to each test based on the  $a/d$ . For example, the designation G1 corresponds to the girder tested with an  $a/d$  of approximately 1. Because two different tests were conducted with an  $a/d$  near 4, these girders are designated G4-1 and G4-2. Figure 6 shows the test configurations.

The load was applied by an actuator through a 1½-in.-thick (38 mm) reinforced neoprene bearing pad at a loading rate of 0.25 kip/sec (1.11 kN/sec). Load cells were used to measure the load under the actuator. Linear variable displacement transducers (LVDTs) were used to measure displacement

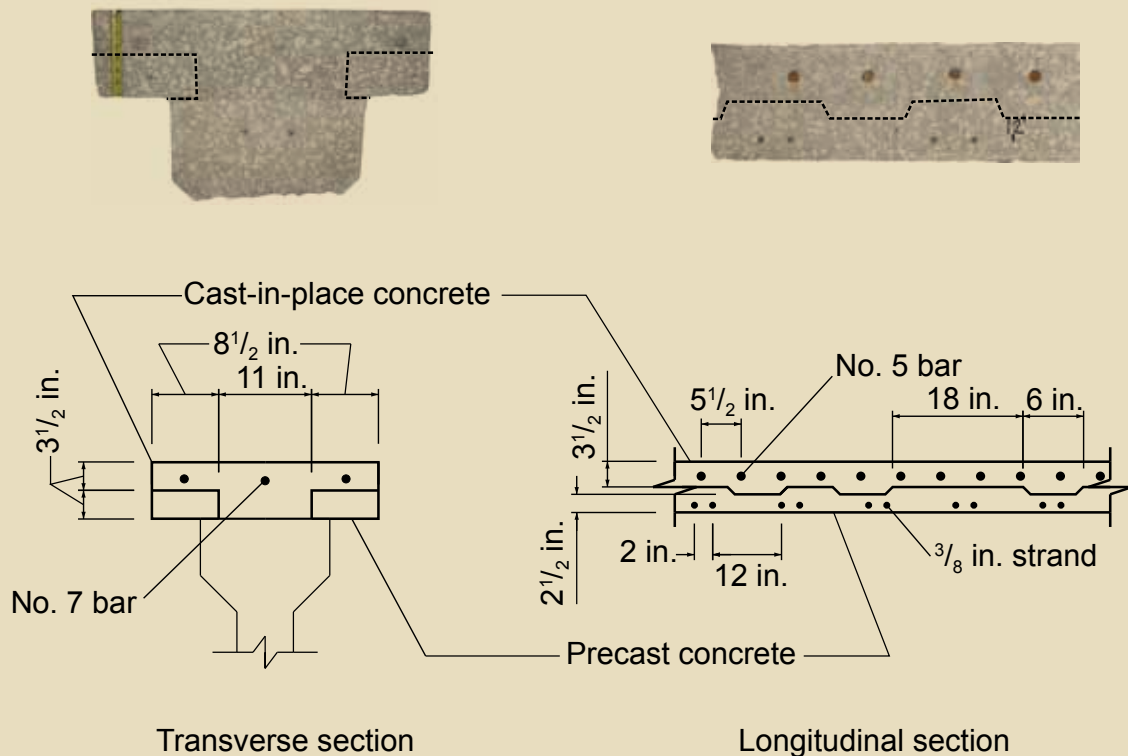


**Figure 4.** The bridge deck used precast concrete slabs under a cast-in-place concrete topping. Note: no. 5 = 16M; no. 7 = 22M; 1 in. = 25.4 mm.

ment at the load point and at each support. LVDTs were also used to monitor any strand slip. Strain was measured at discrete locations using 2.4 in. (60 mm) strain gauges and strain rosettes. This length of gauge has been found appropriate for use in measuring strain in Florida concrete.<sup>9</sup>

## Results and discussion

The results are presented according to the *a/d* used in testing and the corresponding modes of failure, namely bond-shear failure, shear-compression failure, or flexural failure. Discussions of load in this section are presented in terms of superimposed shear, which is defined as the shear between the load point and the nearest support as caused by the actuator. Girder self-weight is not included in the superimposed shear. Furthermore, the displacements presented in the subsequent plots have been corrected for rigid body movement using the measured support displacements and reflect only the deformation of the girder caused by the superimposed load.

The following criteria are used in this paper to categorize girder failure modes. Bond-shear failure is categorized by cracks in the strand development length, slipping of strands, and failure to reach moment capacity. Shear-compression failure is categorized by failure of the compression zone in the shear span due to shear and axial loads. Finally, flexural failure is categorized by crushing of the extreme fiber of the compression zone at the location of maximum moment.

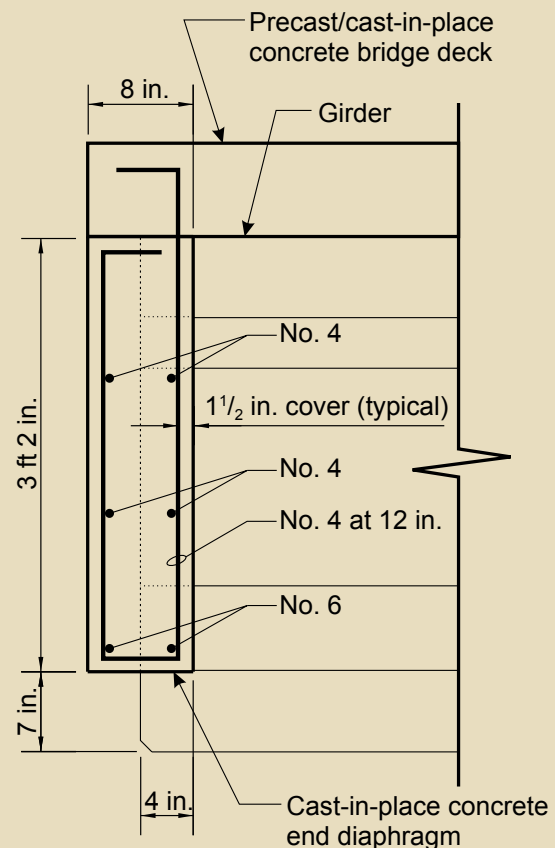


**Figure 5.** The end diaphragms were reinforced cast-in-place concrete. Note: no. 4 = 13M; no. 6 = 19M; 1 in. = 25.4 mm; 1 ft = 0.305 m.

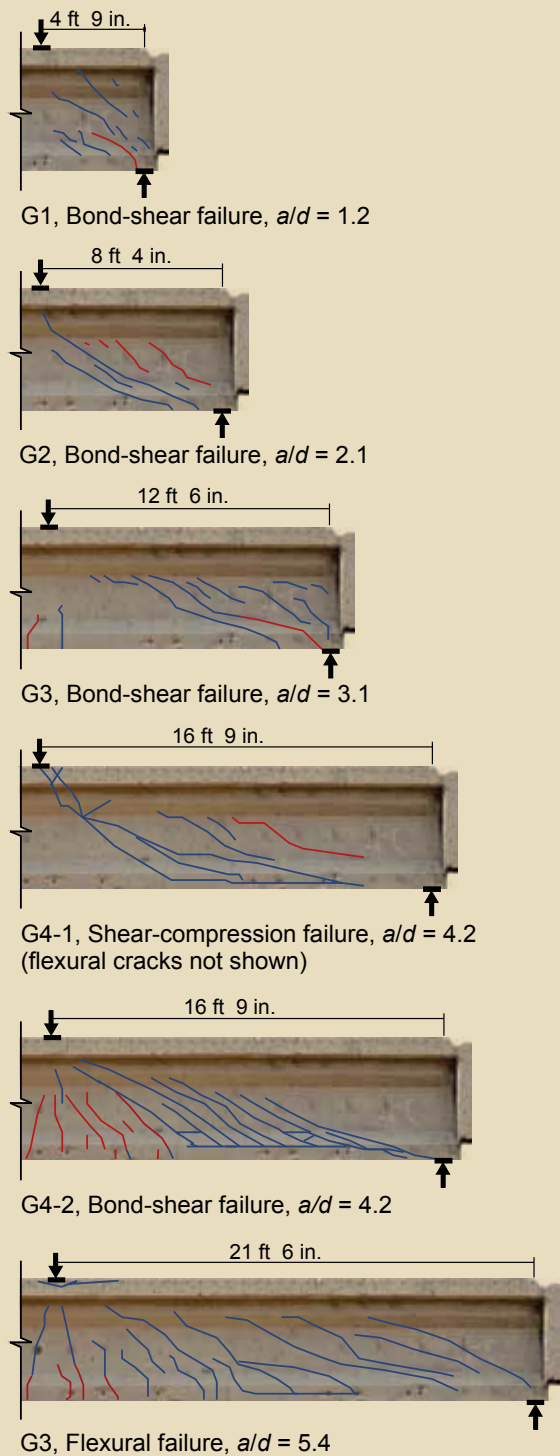


**Figure 6.** Cracking patterns, load location, and failure modes of the test girders. Initial cracks are shown in red, and final cracks are shown in blue. Note:  $a/d$  = shear span-to-depth ratio. 1 in. = 25.4 mm; 1 ft = 0.305 m.

Although the bottom flange contained no confinement reinforcement, no splitting failures were observed in the bottom flange during any test. End diaphragms are believed to have provided confinement necessary to prevent splitting.

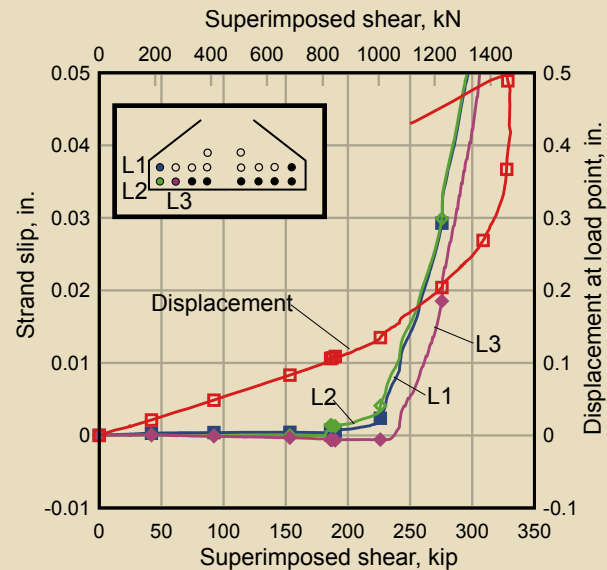


**Figure 7.** Results from girder G1 are representative of girders tested at a shear span-to-depth ratio less than 3.1. Note: 1 in. = 25.4 mm.

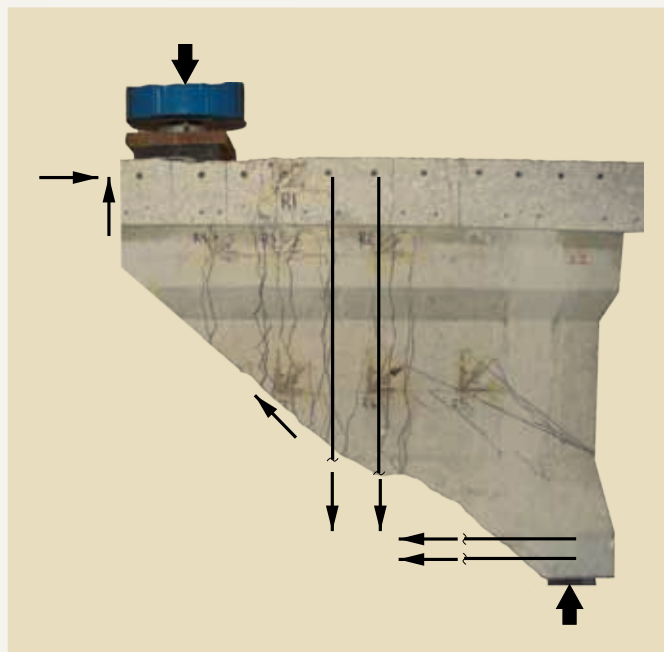


**Figure 8.** Horizontal and vertical mild steel reinforcement contributed to the end-region capacity after cracking.

### Bond-shear failure, $a/d < 3$

Each of the three girders tested at  $a/d$  of 3 or less (G1, G2, and G3) demonstrated bond-shear failure. As previously noted, bond-shear failure is identified by the formation of flexural cracks in the strand development length and by slipping of the strands. The test results of girder G1 are representative of the behavior and failure mode of all three tests and are presented here to demonstrate the behavior accompanying this failure mode.

Girder G1 was tested using an  $a/d$  of 1.2. **Figure 7** shows

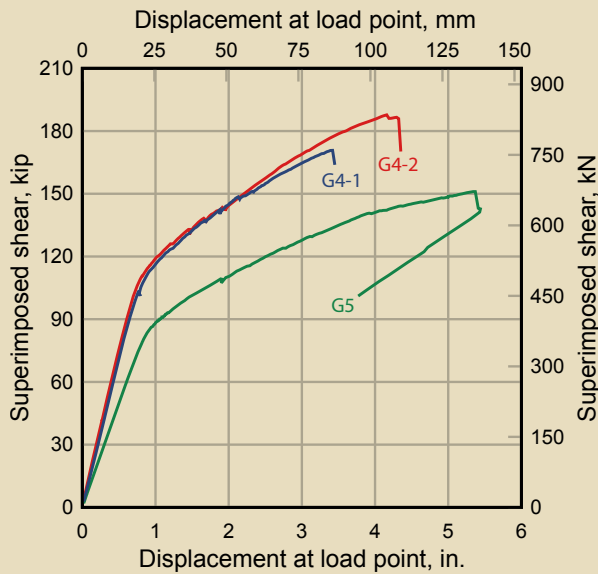


Figure 9. Shear-displacement relationships for girders G4-1, G4-2, and G5.

the shear-displacement response for G1. The girder behaved linear elastically until first cracking, which occurred at 182 kip (810 kN) (Fig. 8). The first crack occurred in the strand development length near the face of the bearing and was confirmed by strain gauges placed in the vicinity of the crack. Cracking reduced the girder stiffness, as apparent in the shear displacement plot. Eventually, the shear reached a maximum load and began to descend, marking the peak capacity of the girder at 331 kip (1470 kN).

Figure 7 also shows a plot of shear versus strand slip for the selected strands. Figure 7 shows a slight slip in the strand at 182 kip (810 kN), the same point at which the first crack formed.

The initial crack that formed near the face of bearing (Fig. 8) significantly reduced the length available for strand development. This loss in development length corresponded with the initial strand slip shown in the plot. The appearance of a crack resulted in the formation of the mechanism in Fig. 8. After the crack formed, rotation of the end region was resisted by the reduced tension capacity of the prestressing strands supplemented by the horizontal and vertical mild steel reinforcement. The girder was able to carry 25% more shear as the strands continued to slip. The shape of the load-deflection diagram indicates that some of the mild steel bars may have been yielding, contributing to the ductile failure mode exhibited.

Although the end-region reinforcement improved the girder's capacity and ductility, it was insufficient to develop the full moment capacity for this short  $a/d$ . If the girder had been constructed without this end-region reinforcement, the continued deformation under this mechanism would have been resisted only by the prestressing strands with a short available development length. Under these condi-

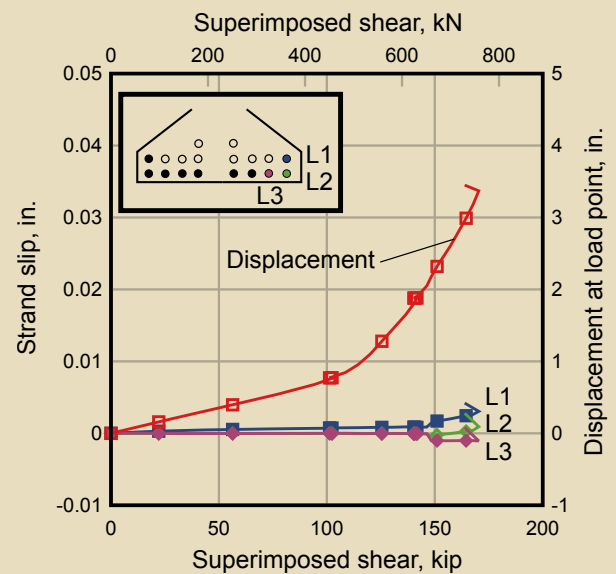


Figure 10. Girder G4-1 had little strand slip. Note: 1 in. = 25.4 mm.

tions it is likely that the girder would have been unable to carry significant additional load beyond the formation of the first crack. The capacity would have depended solely on the slip resistance of the strands between the crack and the girder end. The 2007 AASHTO LRFD Bridge Design Specifications<sup>10</sup> require that the combined tensile capacity of the prestressing strands and longitudinal mild reinforcement be adequate to resist the total horizontal force generated by the end-region mechanism. Results of the tests with  $a/d$  less than or equal to 3 indicate that capacity of the prestressing strands is limited by slipping and that additional capacity beyond this slip point might be possible with the use of vertical and horizontal mild steel reinforcement.

### Shear-compression and bond-shear failure, $a/d = 4$

Two girders were tested with an  $a/d$  of 4.1 (G4-1 and G4-2), each displaying a different mode of failure. Girder G4-1 failed in a shear-compression mode, whereas girder G4-2 failed in a bond-shear mode. Although the girders failed in different manners, their shear versus displacement behavior was similar (Fig. 9). Both girders behaved linear elastically up to a shear load of almost 95 kip (420 kN). Strain gauge data confirmed that cracking occurred in both girders near this load. Above 95 kip, the slopes of the shear-displacement curves began to decrease up to a shear of about 120 kip (534 kN), beyond which the slopes were approximately constant until failure. The slope of the curves between 120 kip and failure corresponds to the stiffness of the cracked girders.

Girder G4-1 failed at a shear of 171 kip (761 kN) due to crushing of the compression zone (Fig. 6), which was accompanied by delamination of the bottom face of the bulb

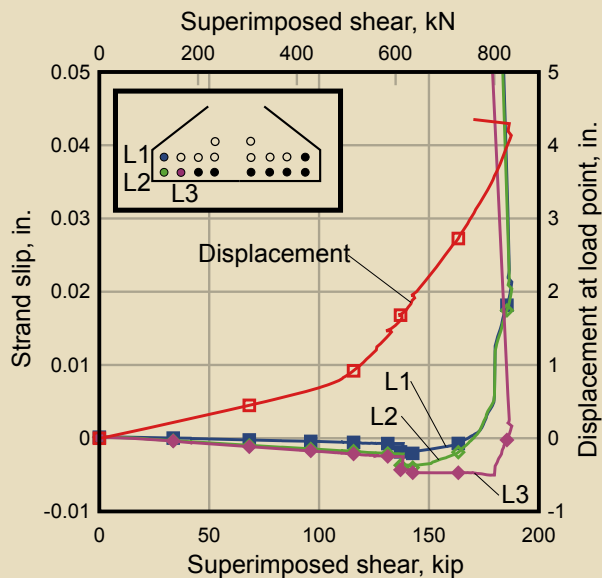


**Figure 11.** Girder G4-2 had significant strand slip leading up to failure. Note: 1 in. = 25.4 mm.

from the girder. The initial web cracks propagated into the compression flange as the load approached failure. These cracks in the compression zone went through the joint between the precast concrete panels and ultimately caused the longitudinal bars in the deck to buckle. Although the strand did slip slightly (Fig. 10), resulting in the mild steel being engaged, the mild steel had sufficient strength to ensure that the capacity was not controlled by strand slip.

Girder G4-2 experienced a bond-shear failure at a shear of 188 kip (836 kN). Based on the test data, it is believed that moderate strand slip began at approximately 130 kip (578 kN). Moderate slip continued until shortly before failure, at which point the strands experienced a drastic and sudden slip. The initial cracks on G4-2 started as flexure cracks (Fig. 6). As the load increased, cracks began to form in the web and then extended toward the support. The

concentration of cracks near the support reduced the strand development length and led to slipping of the strands (Fig. 11). Failure was sudden and resulted in the loss of a portion of the bottom flange.

### Flexural failure, $a/d = 5$

Figure 9 shows the shear versus displacement plot for girder G5. The girder behaved linear elastically until the shear reached 81 kip (360 kN). Initial cracks were flexural and were located under the load point (Fig. 6). Strain gauge data indicated that first cracking occurred at a shear of 72 kip (320 kN) and that cracking did not enter the web until the shear was 89 kip (400 kN). The girder reached a peak shear of 151 kip (672 kN) when the extreme fiber of the compression zone failed near the load point. The failure was categorized as flexure.

Strand slip was insignificant for girder G5. The maximum slip was approximately 0.005 in. (0.12 mm). The girder reached flexural capacity, indicating that sufficient development length was available to develop the full flexural capacity of the section.

### Comparison of results with calculated capacities

Table 1 shows a comparison of the experimental girder capacity with calculated capacities using the following methods:

- modified compression field theory (MCFT) from AASHTO LRFD specifications
- strut-and-tie method (STM) from AASHTO LRFD specifications
- detailed method from American Concrete Institute's (ACI's) *Building Code Requirements for Structural*

**Table 1.** Comparison of calculated shear capacity with experimental results

$a/d$	Test	$V_{EXP}$ kip	MCFT		STM		ACI detailed		Modified end region	
			$V_m$ kip	$\frac{V_{EXP}}{V_n}$	$V_m$ kip	$\frac{V_{EXP}}{V_n}$	$V_m$ kip	$\frac{V_{EXP}}{V_n}$	$V_{nER}$ kip	$\frac{V_{EXP}}{V_n}$
1.2	G1	344	211	1.63	159	2.16	268	1.28	252	1.37
2.1	G2	255	231	1.10	108	2.36	243	1.05	255	1.00
3.1	G3	207	193	1.07	n.a.	n.a.	227	0.91	222	0.93
4.2	G4-1	180	181	0.99	n.a.	n.a.	181	0.99	n.a.	n.a.
4.2	G4-2	198	181	1.09	n.a.	n.a.	181	1.09	n.a.	n.a.
5.4	G5	158	167	0.95	n.a.	n.a.	160	0.99	n.a.	n.a.

Note:  $a/d$  = shear span-to-depth ratio; MCFT = modified compression field theory; n.a. = not applicable; STM = strut-and-tie method;  $V_{EXP}$  = maximum experimental shear capacity;  $V_n$  = nominal shear capacity;  $V_{nER}$  = nominal shear capacity of the end region. 1 kip = 4.448 kN.

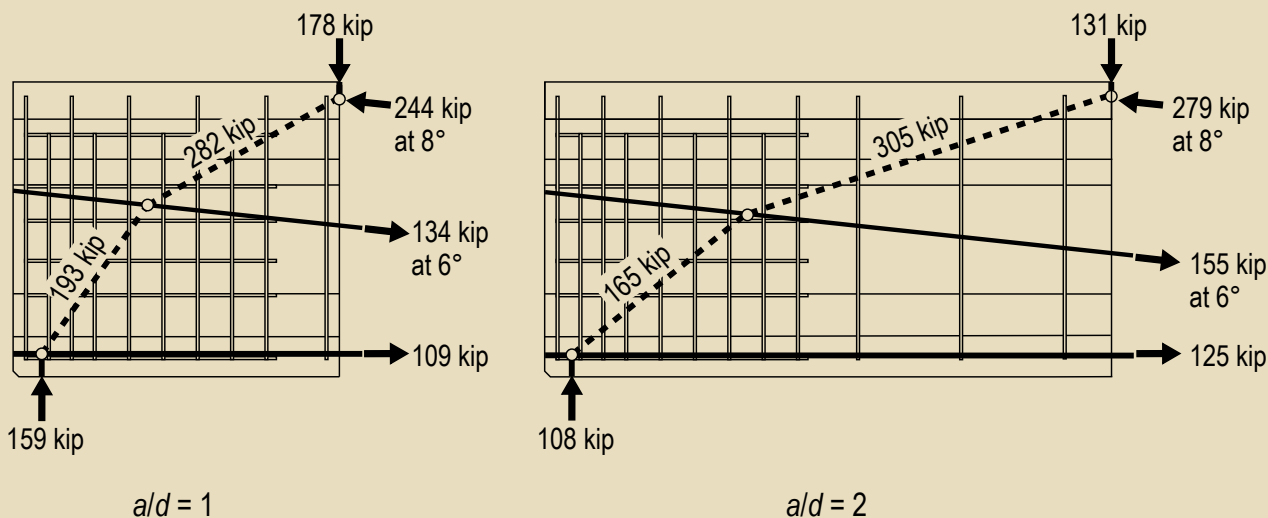


**Figure 12.** Strut-and-tie models for girders G1 and G2. Note:  $a/d$  = shear span-to-depth ratio. 1 kip = 4.448 kN.

*Concrete (ACI 318-08) and Commentary (ACI 318R-08)*<sup>11</sup>

- AASHTO LRFD specifications longitudinal reinforcement (end region) requirement

The failure modes assumed by these methods do not necessarily match those observed in the tests. The comparison, however, gives perspective regarding the predicted versus experimental capacities. Table 1 summarizes the maximum experimental shear capacity  $V_{EXP}$  and predicted nominal shear capacity  $V_n$  for each of the tests. The experimental shear capacities shown in the table include the measured superimposed shear and the calculated shear from self-weight.

The ACI 318-08 and MCFT methods generally provided conservative predictions of shear capacity for all  $a/d$ . Exceptions occurred for the ACI 318-08 prediction with an  $a/d$  of 3.1 and the MCFT prediction with an  $a/d$  of 5.4. Although the predicted capacities for the lower  $a/d$  were reasonable, the failure modes assumed in the models do not match the actual behavior of the girder.

The STM was used to calculate the shear capacity for the tests with an  $a/d$  of 1.2 and 2.1. Strut-and-tie behavior does not control when  $a/d$  is greater than about 2.5, so the method was not used to predict the capacity of girders G3 to G5. **Figure 12** shows the struts, ties, and nodes for the models. The fully bonded straight strands, the harped strands (also fully bonded), and the lowest layer of mild steel were incorporated as ties in the models. For both models, the tie forces controlled the capacity of the STM. This was due, in part, to the short available development length for the prestressing strands in the nodes. The prestressing steel tie capacity was reduced proportionate to the ratio between the available embedded length and the development length predicted by the AASHTO LRFD specifications. The available

development length was determined by assuming a crack between the support and load point.

Both STM models underestimated the girder capacity by more than a factor of two. This is likely due to the enhanced strength contributed by the mild steel bars in the girder end region. In addition, development-length equations are typically conservative, resulting in predicted tie forces that are smaller than the experimental forces. Regardless, the models are considered to represent the lower bound of the girder's shear capacity.

AASHTO LRFD specifications require that the longitudinal steel in the end zone be checked using Eq. (5.8.3.5-2) (Eq. [1]).

$$A_{ps}f_{ps} + A_s f_y \geq \left( \frac{V_u}{\phi_v} - 0.5V_s - V_p \right) \cot \theta \quad (1)$$

where

$A_{ps}$  = area of prestressing steel

$f_{ps}$  = stress in the prestressing steel coincident with  $V_u$

$A_s$  = area of mild steel

$f_y$  = specified yield strength of mild steel

$V_u$  = factored shear force at section under investigation

$\phi_v$  = shear resistance factor

$V_s$  = shear resistance provided by shear reinforcement at section under investigation

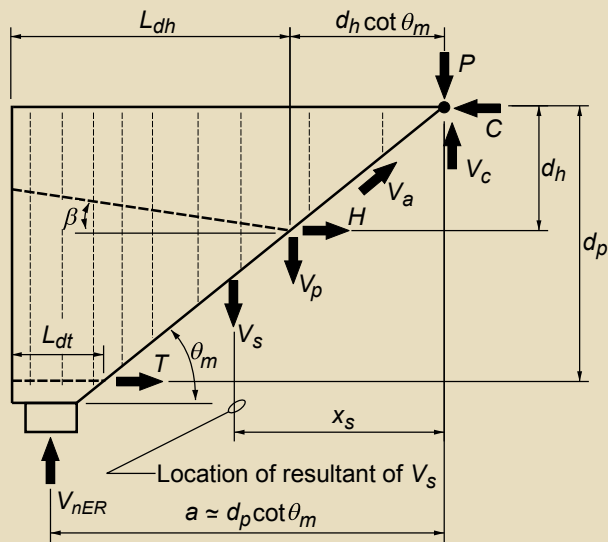


**Figure 13.** End-region model used to calculate shear capacity. Note:  $a$  = shear span;  $C$  = resultant compressive force;  $d_h$  = depth of harped strands at intersection with the inclined section boundary;  $d_p$  = depth of prestressing and mild steel in the bottom tie;  $H$  = capacity of harped strands, accounting for the actual development length;  $L_{dh}$  = available development length of the harped strands;  $L_{dt}$  = available development length of the straight strands;  $P$  = applied load;  $T$  = capacity of prestressing and mild steel in the bottom tie, accounting for the actual development length;  $V_a$  = shear force due to aggregate interlock;  $V_c$  = shear force in concrete compression zone at boundary of shear span;  $V_{nER}$  = nominal shear capacity of the end region;  $V_p$  = effective prestressing force component in the direction of the applied shear;  $V_s$  = shear resistance provided by shear reinforcement at section under investigation;  $x_s$  = distance from the load point to the resultant of  $V_s$ ;  $\beta$  = angle between inclination of the harped strands and the long axis of the member;  $\theta_m$  = angle between the long axis of the member and a line between the support and load point.

$V_p$  = effective prestressing force component in the direction of the applied shear

$\theta$  = angle of inclination of the diagonal compressive stresses

Equation (1) is based on moment equilibrium of the end region and is intended to check that the longitudinal steel in the end region has sufficient capacity to support the tensile force caused by the shear load. It does not, however, consider the variable depth of harped tendons or allow for the variation of transverse reinforcement spacing over the crack length. To accommodate these details, the procedure was modified (Fig. 13):

- The angle of inclination  $\theta_m$  was taken as the angle between the long axis of the girder and a line between the load point and support.
- The actual distribution of transverse mild steel was accounted for by  $x_s$ , which is the distance from the load point to the resultant of  $V_s$ .
- Harped prestressing steel was considered separately.

**Table 2.** Comparison of calculated moment capacity with experimental results

$a/d$	Test	$M_{EXP}$ kip-ft	$M_m$ kip-ft	$\frac{M_{EXP}}{M_m}$
1.2	G1	1641	3072	0.53
2.1	G2	2144	3168	0.68
3.1	G3	2644	3277	0.81
4.2	G4-1	3133	3389	0.92
4.2	G4-2	3420	3389	1.01
5.4	G5	3568	3511	1.02

Note:  $a/d$  = shear span-to-depth ratio;  $M_n$  = nominal moment capacity;  $M_{EXP}$  = maximum experimental moment. 1 kip-ft = 1.356 kN-m.

The equation was rearranged to separate the structural demand (left side) from the structural capacity (right side) to give Eq. (2).

$$V_{nER} \leq \frac{T}{\cot \theta_m} + \frac{Hd_h}{d_p \cot \theta_m} + \frac{V_s x_s}{d_p \cot \theta_m} + \frac{V_p d_h}{d_p} \quad (2)$$

where

$V_{nER}$  = nominal shear capacity of the end region

$T$  = capacity of prestressing and mild steel in the bottom tie, accounting for the actual development length

$\theta_m$  = angle between the long axis of the member and a line between the support and load point

$H$  = capacity of harped strands, accounting for the actual development length

$d_h$  = depth of harped strands at intersection with the inclined section boundary

$d_p$  = depth of prestressing and mild steel in the bottom tie

As with the STM, only the fully bonded straight strands, the harped strands, and the bottom layer of mild steel were assumed to contribute to the end-region capacity. The upper layers of mild steel were not included because they do not always cross the inclined plane in the model and because they have relatively small moment arms about the load point. The stresses in the mild steel and prestressing strands were reduced to reflect the available development length.

The right side of Eq. (2) is taken as the nominal shear capacity predicted for the end region. Table 1 shows the results from this equation. Based on the applicability of the end-region requirements, only the capacities of girders G1, G2, and G3 were calculated. As with the STM, steel tie

capacity was reduced proportionate to the ratio between the available embedded length (Fig. 13) and the development length predicted by the AASHTO LRFD specifications. The end-region predictions, however, were in better agreement with the tested capacity than the STMs. This improvement is attributed to the contribution of the transverse mild steel. Although the capacities calculated using MCFT and ACI 318-08 are also in good agreement, these methods are intended for sectional application and do not reflect the behavior demonstrated by the test girders.

Nominal moment capacity  $M_n$  was calculated using the principles of strain compatibility. **Table 2** summarizes the maximum experimental moment  $M_{EXP}$  at failure for each test and the corresponding nominal moment capacity. The applied moment includes the self-weight of the girder. The following material properties were used to calculate moment capacity:

- The compressive strength of concrete was 5.0 ksi (34.5 MPa).
- Prestress in the strands was 190 ksi (1310 MPa).
- Ultimate tensile strength was assumed to be 286 ksi (1970 MPa).
- Young's modulus for the strands was 28,500 ksi (196.5 GPa).

## Conclusion

Four 30-year-old Type III bridge girders were removed from service and load tested. An approximately 28-in.-wide (710 mm) section of the bridge deck and end diaphragm was retained with each test girder. The bridge deck consisted of precast concrete planks spanning between girders covered by a cast-in-place concrete topping slab. Items of interest included the performance of the bridge deck as the compression flange, the lack of confinement steel around the strands in the end region, the capacity of the girders after 30 years in service, and the mode of failure corresponding to varying  $a/d$ . Tests were conducted using values for  $a/d$  that ranged from 1.2 to 5.4. After testing, concrete and steel samples were taken and tested to confirm material properties. These properties were used to calculate girder capacities as predicted by MCFT, STM, and ACI models. In addition, a modified version of the end-region capacity from the AASHTO LRFD specifications was calculated.

The following conclusions were made:

- Overall, the 30-year-old girders performed well in load tests. The full-scale testing gave no indication of reduced capacity or performance as a result of exposure or use. Testing confirmed visual ratings made during inspections before demolition.

- For an  $a/d$  of 3 or less, the failure mode was bond shear. Strand slip was precipitated by the formation of flexural cracks in the strand development length near the face of the support. It is believed that crack formation engaged the transverse and longitudinal mild steel reinforcement at the girder end and resulted in a 25% greater load than that recorded at the initial strand slip.
- One test that was conducted with an  $a/d$  of 4 resulted in shear-compression failure, whereas the other resulted in bond-shear failure. The change in failure mode between bond-shear failure and shear-compression failure occurs near an  $a/d$  of 4.
- Flexural failure occurred in the single test conducted with an  $a/d$  of 5. The transition to flexural controlled behavior occurred with an  $a/d$  between 4 and 5.
- One of the tests with an  $a/d$  of 4 resulted in extensive crushing of the deck, which included buckling of the longitudinal bars. The crack aligned with one of the joints between the precast concrete panels. The data, however, indicated that the panel system performed adequately compared with that of a cast-in-place concrete deck.
- For tests conducted with a small  $a/d$ , the actual failure mode (bond failure) was different from the mode assumed by the MCFT and ACI 318-08 models. However, the capacities predicted by these models were generally conservative compared with the experimental results.

## Acknowledgments

This paper presents results from FDOT research project contract number BD545-56. The authors would like to acknowledge and thank FDOT for funding this research project. In addition, the authors would like to thank David Allen, Frank Cobb, Steve Eudy, Tony Hobbs, Will Potter, Paul Tighe, and Chris Weigly of the FDOT Structures Research Center in Tallahassee, Fla., for their assistance with the removal and testing of these girders. The authors would also like to thank Gus Llanos, who worked as a research assistant at the University of Florida and helped during testing of the girders.

## References

1. Ma, Z., M. K. Tadros, and M. Baishya. 2000. Shear Behavior of Pretensioned High-Strength Concrete Bridge I-Girders. *ACI Structural Journal*, V. 97, No. 1 (January–February): pp. 185–192.
2. Shahawy, M., B. Robinson, and B. Batchelor. 1993. *An Investigation of Shear Strength of Prestressed Concrete AASHTO Type II Girders*. Tallahassee, FL: Florida Department of Transportation.

3. Kuchma, D., K. Kim, T. Nagle, S. Sun, and N. Hawkins. 2008. Shear Tests on High-Strength Prestressed Bulb-Tee Girders: Strengths and Key Observations. *ACI Structural Journal*, V. 105, No. 3 (May): pp. 358–367.
4. Csagoly, P. 1991. *A Shear Moment Model for Prestressed Concrete Beams*. Tallahassee, FL: FDOT.
5. Kaufman, M., and J. Ramírez. 1988. Re-evaluation of the Ultimate Shear Behavior of High-Strength Concrete Prestressed I-Beams. *ACI Structural Journal*, V. 85, No. 3 (May): pp. 295–303.
6. Deatherage, J., E. Burdette, and C. Chew. 1994. Development Length and Lateral Spacing Requirements of Prestressing Strand for Prestressed Concrete Bridge Girders. *PCI Journal*, V. 39, No. 1 (January–February): pp. 70–83.
7. Llanos, G., B. Ross, and H. Hamilton. 2009. *Shear Performance of Existing Prestressed Concrete Bridge Girders*. Tallahassee, FL: FDOT.
8. American Association of State Highway and Transportation Officials (AASHTO). 1973. *Standard Specifications for Highway Bridges*. 11th ed. Washington, DC: AASHTO.
9. Ross, B., and H. Hamilton. 2011. Evaluation of Strain Gage Lengths for Testing Limestone and Granite Aggregate Concrete. *Construction and Building Materials*, V. 25, No. 1 (January): pp. 406–408.
10. American Association of State Highway and Transportation Officials (AASHTO). 2007. *AASHTO LRFD Bridge Design Specifications*. 4th ed. Washington, DC: AASHTO.
11. American Concrete Institute (ACI) Committee 318. 2008. *Building Code Requirements for Structural Concrete (ACI 318-08) and Commentary (ACI 318R-08)*. Farmington Hills, MI: ACI.

### Notation

- $a$  = shear span
- $ald$  = shear span-to-depth ratio
- $A_{ps}$  = area of prestressing steel
- $A_s$  = area of mild steel
- $C$  = resultant compressive force
- $d$  = depth to the centroid of prestressing strands

- $d_h$  = depth of harped strands at intersection with the inclined section boundary
- $d_p$  = depth of prestressing and mild steel in the bottom tie
- $f_{ps}$  = stress in the prestressing steel coincident with  $V_u$
- $f_y$  = specified yield strength of mild steel
- $H$  = capacity of harped strands, accounting for the actual development length
- $L_{dh}$  = available development length of the harped strands
- $L_{dt}$  = available development length of the straight strands
- $M_{EXP}$  = maximum experimental moment
- $M_n$  = nominal moment capacity
- $P$  = applied load
- $T$  = capacity of prestressing and mild steel in the bottom tie, accounting for the actual development length
- $V_a$  = shear force due to aggregate interlock
- $V_c$  = shear force in concrete compression zone at boundary of shear span
- $V_{EXP}$  = maximum experimental shear capacity
- $V_n$  = nominal shear capacity
- $V_{nER}$  = nominal shear capacity of the end region
- $V_p$  = effective prestressing force component in the direction of the applied shear
- $V_s$  = shear resistance provided by shear reinforcement at section under investigation
- $V_u$  = factored shear force at section under investigation
- $x_s$  = distance from the load point to the resultant of  $V_s$
- $\beta$  = angle between inclination of the harped strands and the long axis of the member
- $\theta$  = angle of inclination of the diagonal compressive stresses
- $\theta_m$  = angle between the long axis of the member and a line between the support and the load point
- $\phi_v$  = shear resistance factor

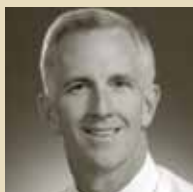
## About the authors



Brandon E. Ross, P.E., is a doctoral candidate in the Department of Civil and Coastal Engineering at the University of Florida in Gainesville, Fla.



Marc Ansley, P.E., served as the director of the Florida Department of Transportation Structures Research Center in Tallahassee, Fla. Ansley died suddenly in June 2010. The Marcus H. Ansley Structures Research Center was dedicated to his memory in December 2010.



H. R. (Trey) Hamilton, PhD, P.E., is an associate professor of civil and coastal engineering at the University of Florida in Gainesville.

## Abstract

Six load tests were conducted on American Association of State Highway and Transportation Officials (AASHTO) Type III girders that were salvaged from an almost 30-year-old bridge. Specimens were tested in three-point bending at shear span-to-depth ratios  $a/d$  ranging from 1.2 to 5.4. Items of interest included the age of the structure, lack of confinement steel as required by *AASHTO LRDF Bridge Design Specifications*, the performance of horizontal and vertical mild steel in the end region, the presence of end diaphragms, and the combination precast/cast-in-place concrete bridge deck.

The results of the testing indicated that the girders had

no ill effects from age or exposure over the 30-year service life. Girders tested with short shear spans ( $a/d \leq 3.1$ ) exhibited a bond-shear failure mode categorized by cracks in the strand development zone, slipping of the strands, and failure to reach moment capacity. Mild steel reinforcement in the end region improved the capacity by 25% beyond the point where strand slip was detected. One of the two girders tested with an  $a/d$  of 4.2 exhibited bond-shear failure, while the other exhibited shear-compression failure. Both failures were abrupt. The single girder tested with an  $a/d$  of 5.4 failed in flexure.

Experimental capacities were compared with sectional models, strut-and-tie models, and the end-region requirement for longitudinal reinforcement in the AASHTO LRFD specifications. The sectional models do not consider the bond-shear failure mode demonstrated by many of the tests but still predicted generally conservative shear capacities. Finally, the performance of the bridge deck was evaluated. The deck consisted of precast concrete planks that spanned between girders and supported a cast-in-place concrete topping slab. No adverse effects from the deck system were observed during testing.

## Keywords

AASHTO, diaphragm, girders, shear span.

## Review policy

This paper was reviewed in accordance with the Precast/Prestressed Concrete Institute's peer-review process.

## Reader comments

Please address any reader comments to [journal@pci.org](mailto:journal@pci.org) or Precast/Prestressed Concrete Institute, c/o *PCI Journal*, 200 W. Adams St., Suite 2100, Chicago, IL 60606. 